

# Robust affine feature matching via quadratic assignment on Grassmannians

Alexander Kolpakov

*Institut de Mathématiques, Université de Neuchâtel, Rue Emile-Argand 11,  
CH-2000 Neuchâtel, Suisse / Switzerland*

Michael Werman

*School of Computer Science and Engineering, The Hebrew University of Jerusalem,  
91904 Jerusalem, Israel*

---

## Abstract

GraNNI (Grassmannians for Nearest Neighbours Identification) a new algorithm to solve the problem of affine registration is proposed. The algorithm is based on the Grassmannian of  $k$ -dimensional planes in  $\mathbb{R}^n$  and minimizing the Frobenius norm between the two elements of the Grassmannian. The Quadratic Assignment Problem (QAP) is used to find the matching. The results of the experiments show that the algorithm is more robust to noise and point discrepancy in point clouds than previous approaches.

---

## 1. Introduction

Affine registration has a long history in computer vision literature, and extensive work was carried out for affine registration in two and three dimensions, [1, 12, 3, 5, 2]. In [4], two interesting matching problems are formulated and solved based on affine registration in higher dimensions; stereo correspondence under motion and image set matching.

This paper is especially related to [9] which proposed a two-stage procedure to recover correspondences between unlabelled, affinely transformed point sets. The first step finds the affine transformation and the second the matching between the point sets. Specifically, we adopt their first step of using the Grassmannian which is invariant under linear (affine) transformations of the point sets.

As noted in [8] it is provably better, in certain cases, to use an *indefinite relaxation* of the Quadratic Assignment Problem (QAP), used to find the

matching, which almost always discovers the optimal permutation, while the common convex relaxation almost always fails.

These theoretical results bring us to propose a relaxed quadratic programming approach to find the correct permutation (match) between the point sets. The experimental results support our idea that the new algorithm is more robust to noise and point discrepancy in point clouds than [9].

## 2. Algorithm GraNNI (Grassmannians for Nearest Neighbours Identification)

Let  $X, Y \subset \mathbb{R}^{d \times n}$  be two  $n$  point clouds in  $\mathbb{R}^d$ , such that  $Y = L X S + t$  for a linear transformation  $L \in \text{GL}(d)$ , a permutation matrix  $S \in \text{Sym}(n)$ , and a translation vector  $t \in \mathbb{R}^d$ . We assume that  $t = 0$  by translating both point clouds to have barycenters at 0. Also we assume, generically, that  $\text{rank } X = d$ , which implies the same rank for  $Y$ .

Let  $\text{Gr}(k, n)$  be the Grassmannian of  $k$ -dimensional planes in  $\mathbb{R}^n$ . We can view the point cloud  $X$  as a map  $X : \mathbb{R}^n \rightarrow \mathbb{R}^d$  defined by  $X(v) = X v$ , for  $v \in \mathbb{R}^n$ . Then  $\ker X$  is an element of  $\text{G} = \text{Gr}(n - d, n) \cong \text{Gr}(d, n)$ . Moreover, for any  $L \in \text{GL}(d)$  we have  $\ker LX = \ker X$ . Thus,  $X$  and all its non-degenerate images define the same element of  $\text{G}$ .

Let  $P_X$  be the orthogonal projection of  $\mathbb{R}^n$  onto  $\ker X$ . The orthogonal projection  $P_X$  which uniquely defines  $\ker X$  will be used as an element of  $\text{G}$ . Note that  $P_X$  can be computed from the singular value decomposition (SVD) of  $X$ .

We also have  $P_Y = S^t P_X S$ . The matrix  $S$  is not unique if there is a linear transformation  $T \in \text{GL}(d)$  such that  $T X = X S$ . Generically this does not happen, which we formulate as “ $X$  has no symmetries”.

Assuming that  $X$  is the “real” point cloud, while noise and missing or added points may affect  $Y$ , we formulate our problem as

$$\min_{S \in \text{Sym}(n)} \|P_Y - S^t P_X S\|_F \iff \max_{S \in \text{Sym}(n)} \text{tr}(P_Y S^t P_X S). \quad (1)$$

This problem is the Quadratic Assignment Problem (QAP) [7] and is known to be NP-complete.

However, the result of [8] suggests that the indefinite relaxation rQAP of QAP suggested in [14] finds the optimal solution  $S_*$  with high probability.

In the ideal case when  $P_Y = S^t P_X S$  we have  $\max_{S \in \text{Sym}(n)} \text{tr} P_Y S^t P_X S = \text{tr} P_Y^2 = \text{tr} P_Y = d$ . Thus, given a matrix  $S$  produced by rQAP, we may assign a weight  $w(S)$  to it that measures the proximity of  $S$  to  $S_*$ . For example,  $w(S) = \exp(-C \cdot (\text{tr}(P_Y S^t P_X S) - d)^2)$  for some large constant

$C > 0$ . The only requirement of  $w(S)$  is that  $w(S) \approx 1$  for permutations  $S$  that are Hamming-close to  $S_*$  and  $w(S) \approx 0$  for all others.

The idea is to run a sufficiently large number  $N \gg 1$  of trials of rQAP, and obtain  $S_1, \dots, S_N$  solutions, and then project

$$\pi : \sum_{i=1}^N w(S_i) S_i \mapsto S_0 \in \text{Sym}(n), \quad (2)$$

where the projection  $\pi$  to the nearest permutation can be realized e.g. by the Hungarian Algorithm.

Once  $S$  is recovered, we can recover  $L$  as

$$L = Y S^T X^T (X X^T)^{-1}, \quad (3)$$

that solves the least squares problem

$$\min_{L \in \text{GL}(d)} \|L X - Y S^T\|_F. \quad (4)$$

#### *Algorithm GraNNI*

*Input:*  $X, Y \in \mathbb{R}^{d \times n}$ , two point clouds such that  $Y = L X S$ , for some unknown  $L \in \text{GL}(d)$  and  $S \in \text{Sym}(n)$ . The number of trials  $N \gg 1$ .

*Assumptions:*  $X$  has rank  $d$  and has no symmetries (generic).

*Output:* Generically,  $S_0 = S$  and  $L_0 = L$ . If  $X$  has symmetries, the output may differ.

*Description:* Perform  $N$  runs of the rQAP indefinite QAP relaxation as described in [14]. Initialize each run randomly. Record the result as  $S_1, \dots, S_N$ . Put  $S_0 := \pi \left( \sum_{i=1}^N w(S_i) S_i \right)$ , where the weight  $w$  and projection  $\pi$  are defined above. Put  $L_0 := Y S_0^T X^T (X X^T)^{-1}$ .

#### *2.1. Correctness*

According to [14], if  $S$  is the result of a single run of GraNNI then  $\mathbb{P}(S = S_*) = 1$ . Thus  $\mathbb{E}[w(S) S] = \mathbb{P}(S = S_*) w(S_*) S_* + \sum_{S \in \text{Sym}(n), S \neq S_*} \mathbb{P}(S' = S) w(S') S' = w(S_*) S_* = S_*$ .

Let us assume that  $w(S') = O\left(\frac{1}{N^k}\right)$ , while  $w(S_*) = 1$ . Also, let  $\tilde{S} = \sum_{i=1}^N w(S_i) S_i$  and  $\bar{S} = \frac{1}{N} \sum_{i=1}^N S_i$ . Moreover, it is reasonable to suppose that  $(S_i)_{kl}$  are i.i.d. for all  $i = 1, \dots, N$  and  $k, l = 1, \dots, n$ . Then we have that

$$\bar{S} = S_* + O\left(\frac{1}{N^{1/2}}\right) \mathbf{1}^T \mathbf{1}, \quad (5)$$

from the Central Limit Theorem.

Let the sample  $\{S_i\}_{i=1}^N$  contain  $m \leq N$  matrices  $S_i = S_*$  and  $N - m \geq 0$  matrices  $S_i \neq S_*$ . Then

$$\tilde{S} = m S_* + \sum_{S_i \neq S_*} O\left(\frac{1}{N^k}\right) S_i = m S_* + O\left(\frac{1}{N^{k-1}}\right) \sum_{S_i \neq S_*} \frac{1}{N} S_i = \quad (6)$$

$$= m S_* + O\left(\frac{1}{N^{k-1}}\right) \left(\bar{S} - \frac{m}{N} S_*\right) = \quad (7)$$

$$= m S_* + O\left(\frac{1}{N^{k-1}}\right) \left(S_* \left(1 - \frac{m}{N}\right) + O\left(\frac{1}{N^{1/2}}\right) \mathbf{1}^T \mathbf{1}\right) = \quad (8)$$

$$= N \mathbb{P}(S_i = S_*) S_* + O\left(\frac{1}{N^{k-1}}\right) \left(\mathbb{P}(S_i \neq S_*) S_* + O\left(\frac{1}{N^{1/2}}\right) \mathbf{1}^T \mathbf{1}\right), \quad (9)$$

where all probabilities are sample probabilities for the sample  $\{S_i\}_{i=1}^N$ .

In order to have  $\pi(\tilde{S}) = S_*$  for any given sample  $\{S_i\}_{i=1}^N$  it would be enough to have

$$\frac{\mathbb{P}(S_i = S_*)}{\mathbb{P}(S_i \neq S_*)} \gg O\left(\frac{1}{N^k}\right), \quad (10)$$

for some  $k \geq 1$  and sufficiently large  $N \gg 1$ . The latter can be achieved by choosing

$$C = \frac{k \log N}{4d^2} \quad (11)$$

in the equality  $w(S) = \exp(-C \cdot (\text{tr}(P_Y S^t P_X S) - d)^2)$ . Indeed, the Cauchy-Bunyakovsky inequality provides

$$|\text{tr}(P_Y S^t P_X S)| \leq \|P_X\|_F \|P_Y\|_F = d, \quad (12)$$

which implies the claim.

## 2.2. Robustness to noise

As follows from Wedin's theorem [15] (see also Theorem 2.5 and Corollary 2.6 in [11]), given two point clouds  $X, Y \subset \mathbb{R}^{d \times n}$  any small perturbation of the vectors in  $Y$  results only in a small perturbation of the projections  $P_X$  and  $P_Y$  as the subspaces  $\ker X^\perp$ , resp.  $\ker Y^\perp$ , correspond to the  $d$  largest singular values of  $X$ , resp.  $Y$ . This means that  $\ker Y$  is only slightly perturbed in the sense that if  $\tilde{Y} = Y + N$ , where  $N$  represents noise, then  $\|P_Y - P_{\tilde{Y}}\|_2 = O(\|N\|_2)$ .

### 2.3. Point discrepancy

Let  $X \subset \mathbb{R}^{d \times m}$  and  $Y \subset \mathbb{R}^{d \times n}$  where  $m < n$  and there exist  $L \in \text{GL}(d)$  and  $S \in \{0, 1\}^{n \times m}$  such that  $Y' = Y S = L X$ .

Then we replace the projection matrix  $P_X \in \mathbb{R}^{m \times m}$  with  $P_X \leftarrow P_X \oplus \mathbf{0}_{n-m}$  and apply GraNNI to the new pair  $P_X, P_Y \in \mathbb{R}^{n \times n}$ . Once an output  $S_0$  is produced, we pick only the first  $m$  columns to produce a matching between the points of  $X$  and  $Y$ . Indeed, matching any of the extra  $n - m$  rows / columns of  $P_Y$  to a zero row / column in  $P_X$  will be heavily penalized, and thus rQAP will target the closest possible match for the first  $m$  rows / columns of  $P_X$  and some  $m$  rows / columns of  $P_Y$ . Based on our numerical result this approach works well with missing / added points in  $X$  and  $Y$  even for relatively large discrepancies.

## 3. Numerical experiments

In our numerical experiments, GraNNI was applied to the following point clouds: specimen cloud  $X \subset \mathbb{R}^{3 \times m}$  and  $Y \subset \mathbb{R}^{3 \times n}$  such that

- $X$  is a random subset of  $X' \subset \mathbb{R}^{3 \times n}$  with  $m = \lfloor \lambda n \rfloor$  points with  $\lambda \in (0, 1]$  being the level of similarity (with  $\lambda = 1$  if all of  $X$  coincides with  $X'$ );
- $Y = Y' \odot N$ , with  $Y' = L X' S$ ,  $L \in \text{GL}(3)$  a random linear map such that  $L = P O$  with  $P$  a positive definite matrix having condition number  $c \in [1, +\infty)$  and  $O$  a uniformly distributed orthogonal matrix;  $S \in \text{Sym}(n)$  a random permutation; and  $N$  being multiplicative noise such that  $N_{ij} \in \mathcal{N}(1, \sigma^2)$ ,  $i = 1, \dots, 3$ ,  $j = 1, \dots, n$ , are i.i.d. Gaussian variables. Here  $\odot$  means the Hadamard (entry-wise) matrix product.

The following quantities were recorded in each experiment:

- the error in recovering  $L$  defined as  $\delta_L = \|L - L_0\|_2 / \|L\|_2$ ;
- the error in matching the preimages defined as  $\delta_X = \|[L_0^{-1} Y S^T]_X - X\|_2 / \|X\|_2$ , where  $[A]_B$  means the matrix formed from the columns of  $A = L_0^{-1} Y S^T \in \mathbb{R}^{d \times n}$  indexed with the same indexes as the columns of  $B = X \in \mathbb{R}^{d \times m}$  inside  $X' \in \mathbb{R}^{d \times n}$ ;
- the error in matching the images defined as  $\delta_Y = \|L X - L_0 X\|_2 / \|L X\|_2$ .

We used the following values for  $\sigma$  (noise level) and  $\lambda$  (similarity level to create point discrepancy):

- $\sigma \in \{0.0, 0.01, 0.05, 0.1, 0.15, 0.2\}$ ,
- $\lambda \in \{1.0, 0.95, 0.90, 0.85, 0.8, 0.7, 0.6, 0.5\}$ .

It appears to us that there is no need to increment  $\sigma$  uniformly as we need to test only for reasonably small levels of noise (to observe that the algorithm works robustly) and for relatively high ones (to conclude about the limits of the algorithm’s applicability). It also appears that we do not need to use lower levels of similarity than 0.5 as likely more than half of the points missing constitutes a fairly large discrepancy. As in the case of noise, we prefer to vary the discrepancy non-uniformly.

The Python code to perform the tests and the respective output stored in separate files is accessible on GitHub [6]. The code requires SageMath [13] and runs in the Jupiter environment. The output data is saved in `csv` format and can be accessed without the need to run the code first.

To support our theoretical findings, numerical experiments were run with the (unoccluded) Caerbannog clouds [10] as the initial source of test examples. For each value of the noise  $\sigma$  and point discrepancy  $\lambda$  a batch of 10 tests was run and the mean values of  $\delta_L$ ,  $\delta_Y$ , and  $\delta_X$  were computed. Every run of GraNNI used  $N = 2^{10}$  calls to rFAQ.

Below we provide a graphical interpretation of the results, where for each value of  $\sigma$  the values of  $\delta_*$ ,  $*$   $\in \{L, X, Y\}$  are provided for different values of  $\lambda$ . The higher the point discrepancy (i.e. the lower  $\lambda$ ), the longer the horizontal bar over the respective value of  $\delta_*$ ,  $*$   $\in \{L, X, Y\}$ .

In Figures 1 – 8, we provide only values  $\delta_* \leq 1.5$ , and sometimes cannot avoid the visual merging and overlaps of some of the horizontal bars. The exact values of  $\delta_*$ ,  $*$   $\in \{L, X, Y\}$  can be found in the dedicated GitHub repository [6].

As part of the data available in [6], we also measured the quantities

1.  $d_\sigma = \|Y' - Y\|_2 / \|Y\|_2$  (the relative noise as compared to the ground truth image of  $X$  under  $L$ ); and
2.  $d_\lambda = \|X' \setminus X\|_2 / \|X\|_2$  (the relative point discrepancy as compared to the initial specimen image).

The `csv` files of the test data contain the following values in each line exactly in this order:  $\sigma$ ,  $\lambda$ ,  $d_\sigma$ ,  $d_\lambda$ ,  $\delta_L$ ,  $\delta_Y$ ,  $\delta_X$ . We are mostly interested in measuring  $\delta_L$  and  $\delta_Y$  to understand how well we can recover  $L$  and how well the recovered linear map  $L_0$  approximates the original image of  $X$  under the action of  $L$ . The distance between the preimage of  $Y$  under  $L_0$  and the specimen image  $X$  is used for comparison, and we use preimages for

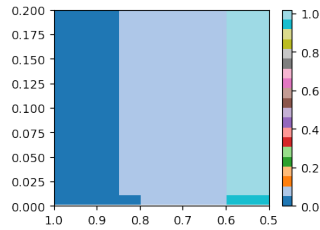


Figure 1: “Teapot” cloud:  $\delta_L$  as a function of  $\lambda$  (discrepancy level, horizontal) and  $\sigma$  (noise level, vertical)

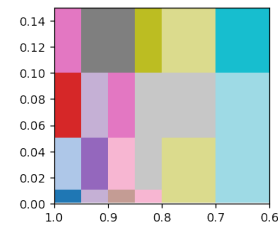


Figure 2: “Teapot” cloud:  $\delta_X$  as a function of  $\lambda$  (discrepancy level, horizontal) and  $\sigma$  (noise level, vertical)

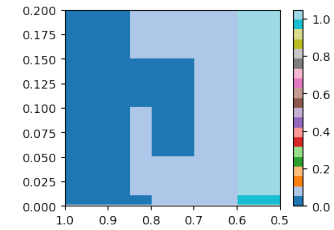


Figure 3: “Teapot” cloud:  $\delta_Y$  as a function of  $\lambda$  (discrepancy level, horizontal) and  $\sigma$  (noise level, vertical)

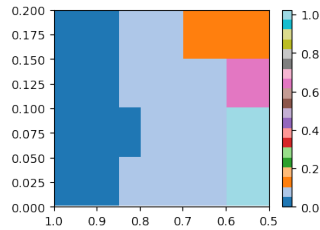


Figure 4: “Bunny” cloud:  $\delta_L$  as a function of  $\lambda$  (discrepancy level, horizontal) and  $\sigma$  (noise level, vertical)

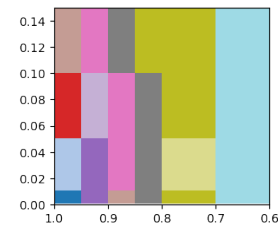


Figure 5: “Bunny” cloud:  $\delta_X$  as a function of  $\lambda$  (discrepancy level, horizontal) and  $\sigma$  (noise level, vertical)

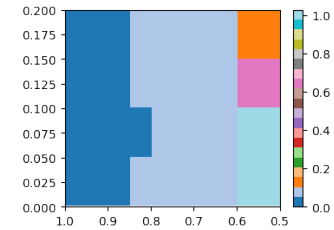


Figure 6: “Bunny” cloud:  $\delta_Y$  as a function of  $\lambda$  (discrepancy level, horizontal) and  $\sigma$  (noise level, vertical)

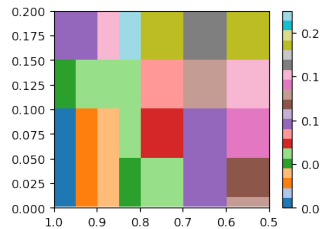


Figure 7: “Cow” cloud:  $\delta_L$  as a function of  $\lambda$  (discrepancy level, horizontal) and  $\sigma$  (noise level, vertical)

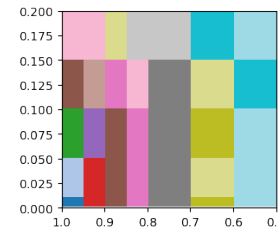


Figure 8: “Cow” cloud:  $\delta_X$  as a function of  $\lambda$  (discrepancy level, horizontal) and  $\sigma$  (noise level, vertical)

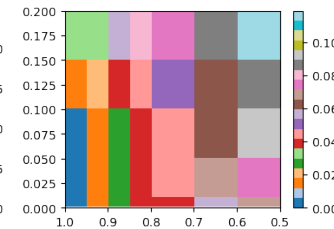


Figure 9: “Cow” cloud:  $\delta_Y$  as a function of  $\lambda$  (discrepancy level, horizontal) and  $\sigma$  (noise level, vertical)

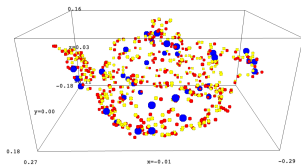


Figure 10: “Teapot” cloud: specimen  $X$  (yellow), preimage of  $L_0^{-1} Y$  (yellow), and point discrepancy between (blue).

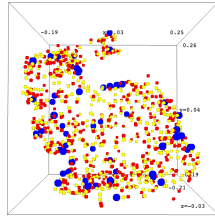


Figure 11: “Bunny” cloud: specimen  $X$  (yellow), preimage of  $L_0^{-1} Y$  (yellow), and point discrepancy between (blue)

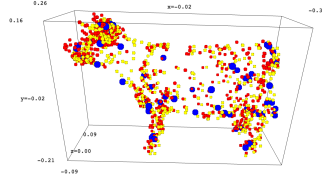


Figure 12: “Cow” cloud: specimen  $X$  (yellow), preimage of  $L_0^{-1} Y$  (yellow), and point discrepancy between (blue)

illustrative purposes (as the direct images under  $L$  can be fairly deformed and thus less suitable for visualization).

The linear transformation  $L$  in all tests had condition number  $\text{cond } L = \|L\|_2 \|L^{-1}\|_2$  equal to 3.

In Figures 10, 11 and 12 we show the specimen cloud  $X$  (yellow), the preimage  $[L^{-1} Y S^T]_X$  (red), and also the point discrepancy consisting of points in  $X'$  that do not belong to  $X$  (blue). For all three point clouds we have  $\sigma = 0.05$ ,  $\lambda = 0.90$ ,  $\text{cond } L = 3$ . The number of trials in each case is  $N = 2^{10}$ .

In Figure 10 we illustrate a test with  $X$  having 315 points and  $Y$  having 351 points. The test parameters are  $d_\sigma \approx 0.045$ ,  $d_\lambda \approx 0.328$ , with the output  $\delta_L \approx 0.045$ ,  $\delta_Y \approx 0.042$ , and  $\delta_X \approx 0.140$ .

In Figure 11 we illustrate a test with  $X$  having 475 points and  $Y$  having 528 points. The test parameters are  $d_\sigma \approx 0.044$ ,  $d_\lambda \approx 0.306$ , with the output  $\delta_L \approx 0.053$ ,  $\delta_Y \approx 0.044$ , and  $\delta_X \approx 0.127$ .

In Figure 12 we illustrate a test with  $X$  having 541 points and  $Y$  having 602 points. The test parameters are  $d_\sigma \approx 0.048$ ,  $d_\lambda \approx 0.348$ , with the output  $\delta_L \approx 0.036$ ,  $\delta_Y \approx 0.036$ , and  $\delta_X \approx 0.141$ .

#### 4. Comparison to other algorithms

In this section we compare GraNNI to another algorithm, GrassGraf [9], that appears to be state-of-the-art compared to other algorithms used to recover affine correspondences.



We implemented GrassGraph as described by its authors in [9] and applied it in the simplest case of two point clouds  $X, Y \subset \mathbb{R}^{d \times n}$  where  $X$  is the specimen cloud that has to be compared to  $Y = L X S$  with  $L \in \text{GL}(d)$ ,  $S \in \text{Sym}(n)$ .

The main finding is that GrassGraf loses precision very quickly if  $Y$  is affected even by relatively small noise. The test point clouds that were used are the unoccluded Caerbannog clouds [10]. We measured the values  $\delta_L$  and  $\delta_Y$ , just as in the case of GraNNI. These values are already enough to conclude that GrassGraph does not appear to recover  $L$  robustly.

In Figures 13 – 18 we show the graphical depiction of our test results (in the manner analogous to the case of GraNNI) for GrassGraph with 3 Laplacian eigenvectors used. The analogous dataset with test results for GrassGraph with 10 Laplacian eigenvectors used is available on GitHub [6]. We do not reproduce it here as it appears to show only a marginal improvement.

Also, some images of the test clouds are available on GitHub [6]: we do not reproduce them here, just note that the “Teapot” cloud shows slightly better robustness to noise and point discrepancy while, say, the “Cow” cloud already demonstrates a great difference between the recovered  $L_0$  and the initial  $L$  even for relatively small noise and point discrepancy.

## 5. Conclusions

Feature matching is at the heart of many applications and requires robust methods for recovery of correspondences and estimation of geometric transformations between domains.

This paper provides a robust and efficient algorithm to find correspondences between point clouds up to an affine transformation and gives bounds on the robustness of the algorithm in the presence of noise and point discrepancies.

*Acknowledgements.* The authors are grateful to the Department of Computer Science, University of Neuchâtel, for the opportunity to use their computational cluster Phi-2 for the numerical experiments.

*Funding.* This work was supported by the Swiss National Science Foundation [grant no. PP00P2-202667] and by an Israel Science Foundation (ISF) grant.

## References

- [1] Pablo Barrios, Vicente Guzman, and Martin Adams. Pso-cola: A robust solution for correspondence-free point set registration. In *2022 11th International Conference on Control, Automation and Information Sciences (ICCAIS)*, pages 223–230. IEEE, 2022.
- [2] E. Begelfor and M. Werman. Affine invariance revisited. In *2006 IEEE Computer Society Conference on Computer Vision and Pattern Recognition (CVPR'06)*, volume 2, pages 2087–2094, 2006.
- [3] P.J. Besl and Neil D. McKay. A method for registration of 3-D shapes. *IEEE Transactions on Pattern Analysis and Machine Intelligence*, 14(2):239–256, 1992.
- [4] Yu-Tseh Chi, S. M. Nejhun Shahed, Jeffrey Ho, and Ming-Hsuan Yang. Higher dimensional affine registration and vision applications. In David Forsyth, Philip Torr, and Andrew Zisserman, editors, *Computer Vision – ECCV 2008*, pages 256–269, Berlin, Heidelberg, 2008. Springer Berlin Heidelberg.
- [5] Xiaoshui Huang, Guofeng Mei, Jian Zhang, and Rana Abbas. A comprehensive survey on point cloud registration. *arXiv preprint arXiv:2103.02690*, 2021.
- [6] A. Kolpakov and M. Werman. SageMath worksheets for GraNNI: Python code, numerical tests, and test statistics. <https://github.com/sashakolpakov/granni>, 2023.
- [7] Tjalling C Koopmans and Martin Beckmann. Assignment problems and the location of economic activities. *Econometrica: journal of the Econometric Society*, pages 53–76, 1957.
- [8] Vince Lyzinski, Donniell E. Fishkind, Marcelo Fiori, Joshua T. Vogelstein, Carey E. Priebe, and Guillermo Sapiro. Graph matching: Relax at your own risk. *IEEE Transactions on Pattern Analysis and Machine Intelligence*, 38(1):60–73, 2016.
- [9] Mark Moyou, Anand Rangarajan, John Corring, and Adrian M. Peter. A grassmannian graph approach to affine invariant feature matching. *IEEE Transactions on Image Processing*, 29:3374–3387, 2020.

- [10] S. Raghupathi, N. Brunhart-Lupo, and K. Gruchalla. Caerbannog point clouds. National renewable energy laboratory. <https://data.nrel.gov/submissions/153>, 2020.
- [11] G. W. Stewart. Error and perturbation bounds for subspaces associated with certain eigenvalue problems. *SIAM Review*, 15(4):727–764, 1973.
- [12] Lisa Tang, Ghassan Hamarneh, and K Iniewski. Medical image registration: A review. *Medical imaging: technology and applications*, 1:619–660, 2013.
- [13] The Sage Developers. Sagemath, the Sage Mathematics Software System (Version 9.7.1), 2022. <https://www.sagemath.org>.
- [14] Joshua T. Vogelstein, John M. Conroy, Vince Lyzinski, Louis J. Poddrazik, Steven G. Kratzer, Eric T. Harley, Donniell E. Fishkind, R. Jacob Vogelstein, and Carey E. Priebe. Fast approximate quadratic programming for graph matching. *PLOS ONE*, 10(4):e0121002, 2015.
- [15] Per-Åke Wedin. Perturbation bounds in connection with singular value decomposition. *BIT Numerical Mathematics*, 12(1):99–111, 1972.

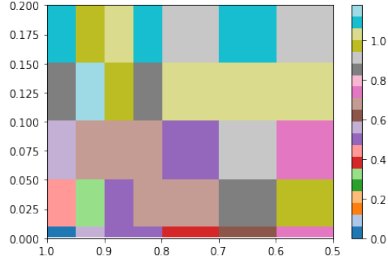


Figure 13: “Teapot” cloud for Grass-Graph:  $\delta_L$  as a function of  $\lambda$  (discrepancy level, horizontal) and  $\sigma$  (noise level, vertical)

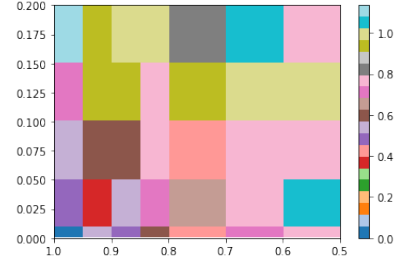


Figure 14: “Teapot” cloud for Grass-Graph:  $\delta_Y$  as a function of  $\lambda$  (discrepancy level, horizontal) and  $\sigma$  (noise level, vertical)

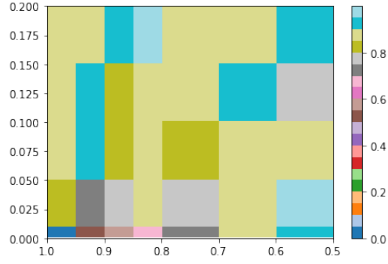


Figure 15: “Bunny” cloud for Grass-Graph:  $\delta_L$  as a function of  $\lambda$  (discrepancy level, horizontal) and  $\sigma$  (noise level, vertical)

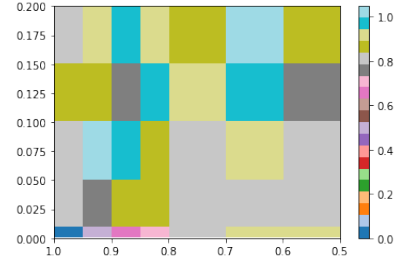


Figure 16: “Bunny” cloud for Grass-Graph:  $\delta_Y$  as a function of  $\lambda$  (discrepancy level, horizontal) and  $\sigma$  (noise level, vertical)

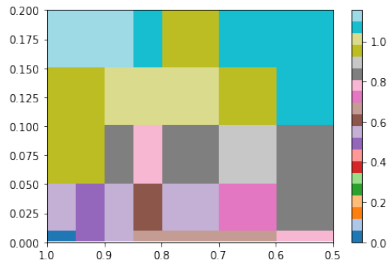


Figure 17: “Cow” cloud for Grass-Graph:  $\delta_L$  as a function of  $\lambda$  (discrepancy level, horizontal) and  $\sigma$  (noise level, vertical)

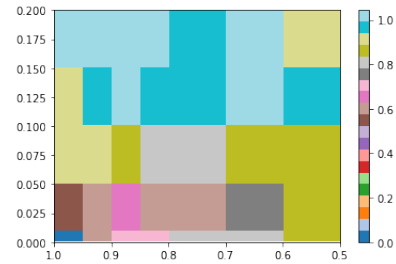


Figure 18: “Cow” cloud for Grass-Graph:  $\delta_Y$  as a function of  $\lambda$  (discrepancy level, horizontal) and  $\sigma$  (noise level, vertical)